scientific reports

Check for updates

OPEN

The role of puff volume in vaping emissions, inhalation risks, and metabolic perturbations: a pilot study

Jennifer Jeon[1,3], Xiaojia He[1,3], Akshada Shinde[2], Maureen Meister[1], Lillie Barnett[1], Qian Zhang[1], Marilyn Black[1], Jonathan Shannahan[2]✉ & Christa Wright[1]✉

Secondhand vaping exposure is an emerging public health concern that remains understudied. In this study, saliva and exhaled emissions from ENDS users (secondhand) and non-ENDS users (baseline) were collected, firsthand emissions were generated using an automated ENDS aerosol generation system programmed to simulate puffing topography profiles collected from ENDS users. Particulate concentrations and sizes along with volatile organic compounds were characterized. We revealed puffing topography metrics as potential mediators of firsthand and secondhand particle and chemical exposures, as well as metabolic and respiratory health outcomes. Particle deposition modeling revealed that while secondhand emissions displayed smaller deposited mass, total and pulmonary particle deposition fractions were higher than firsthand deposition levels, possibly due to smaller secondhand emission particle diameters. Lastly, untargeted metabolomic profiling of salivary biomarkers of lung injury due to firsthand ENDS exposures revealed potential early indicators of respiratory distress that may also be relevant in bystanders exposed to secondhand vaping scenarios. By leveraging system toxicology, we identified 10 metabolites, including leukotriene D4, that could potentially serve as biomarkers for ENDS use, exposure estimation, and the prediction of vaping-related disease. This study highlights characterization of vaping behavior is an important exposure component in advancing our understanding of potential health effects in ENDS users and bystanders.

Keywords Secondhand vaping, ENDS, VOC, Lung health, Metabolomics, Aerosols

Electronic nicotine delivery systems (ENDS) are devices that use an electric current instead of tobacco combustion to vaporize nicotine-containing e-liquids for a user to inhale. Since their commercial release in 2003, ENDS have been marketed as smoking cessation tools and safer alternatives to conventional cigarettes because they emit lower, yet detectible levels of carcinogens, ultrafine particles, and other lung irritants[1]. With the advent of concealable USB-like designs and flavors such as fruit, menthol, and candy[2], ENDS rapidly became the most popular nicotine delivery product used by adolescents in the U.S.[3]. From 2011 to 2015, ENDS use increased by 900% in U.S. middle schoolers and high schoolers, prompting the U.S. Food and Drug Administration (FDA) and the U.S. Surgeon general to declare a youth vaping epidemic[4,5].

In response to the vaping epidemic, the National Academies of Sciences, Engineering, and Medicine (NASEM) and the U.S. Surgeon General published reports calling for research to characterize ENDS aerosol constituents, which are largely unknown due to the lack of U.S. FDA regulation before 2016 and no current testing standards for acceptable emissions[6,7]. Since then, volatile organic compounds (VOCs), heavy metals, and ultrafine particles have been detected in ENDS emissions across multiple devices and e-liquids[1,8–10]. Importantly, ENDS have been shown to release higher concentrations of ultrafine particles relative to conventional cigarettes, and at levels exceeding health-based limits[8,11–13]. This is concerning given ultrafine particles can penetrate deep into the respiratory tract and act as carriers for toxic chemicals to enter the blood stream[12]. Additionally, the Flavor and Extract Manufacturers Association (FEMA) has identified over 1000 flavorings commonly used in e-liquids that may pose a respiratory hazard due to possible volatility and irritant properties[14]. Not surprisingly, International Agency for Research on Cancer (IARC) group 1 and 2 carcinogens, including acrolein, acetaldehyde, formaldehyde, and

[1]Chemical Insights Research Institute of UL Research Institutes, Marietta, GA 30367, USA. [2]School of Health Sciences, Purdue University, West Lafayette, IN 47907, USA. [3]These authors contributed equally: Jennifer Jeon and Xiaojia He. ✉email: jshannah@purdue.edu; Christa.Wright@ul.org

benzene, have been detected in ENDS emissions[12,15,16]. Several of these VOCs are also associated with respiratory infections and lung diseases such as chronic obstructive pulmonary disease (COPD) and asthma[17–19]. Therefore, regardless of how ENDS compare to conventional cigarettes, ENDS emit potentially hazardous toxicants, making their impact on respiratory health a critical question of utmost importance to public safety.

In contrast to primary exposure, little is known about the health effects of inhaling secondhand ENDS aerosols, which are created when an ENDS user exhales near bystanders or non-users. This is particularly concerning because bystanders are exposed to many of the same potentially toxic ultrafine particles, VOCs, and metals that are present in firsthand emissions according to the World Health Organization (WHO)[20]. Importantly, ENDS usage in indoor workplaces and public enclosed places is unregulated in several countries, as well as the majority of U.S. states[20–22], enhancing the risk of unintentional exposure. Using the U.S. EPA unacceptable risk measurements for long-term exposure, the WHO recently concluded formaldehyde and acetaldehyde concentrations presented excess lifetime cancer risk, and concentrations of particulate matter (PM) increased mortality risk in exposed populations. Moreover, indoor particulate matter emission rates from secondhand ENDS emissions exceeded those from secondhand cigarette smoke in some studies, and secondhand particulate matter at vaping conventions reached a level of 12 times higher than the U.S. EPA 24-h standard[12,13]. Still, several gaps remain in the literature on ENDS secondhand emissions. For example, most studies to-date use smoking machines and fail to distinguish the impact of different devices and vaping topographies on indoor air quality[19,23–27]. Because the physicochemical profile of firsthand aerosols varies across ENDS devices, e-liquids, and vaping topographies, future studies are needed that make these same comparisons for secondhand emissions in diverse populations, especially as ENDS devices continue to evolve. These gaps are a prevailing barrier to our understanding of the short- and long-term human health impact of ENDS on bystanders.

To address these knowledge gaps, the present study characterizes the levels of particles and VOCs present in firsthand and secondhand emissions from ten established ENDS devices and users, respectively. We characterized the impact of puffing topography on emissions and found the ENDS users puff volume and flow rate are powerful mediators of firsthand and secondhand particle and chemical exposures. Using computational modeling, we showed substantial particle deposition and VOC inhalation risks for ENDS users, youth, and adult bystanders. Furthermore, untargeted high-resolution metabolomic analysis of saliva from ENDS users revealed firsthand emission exposures elicited unique profiles of lung injury biomarkers associated with asthma and lung cancer pathogenesis. Taken together, these results demonstrate the importance of vaping behavior such as puff volume in mediating particle and chemical exposures, as well as metabolic and respiratory health outcomes in individuals exposed to firsthand and secondhand ENDS emissions.

Materials and methods

Participant recruitment strategy and procedures

This human subject study was approved by Advarra Institutional Review Board (IRB Protocol No. H22081). All methods performed in this study, including recruitment, informed consent, and human data collection, was carried out in accordance with the approved IRB protocol (No. H22081). We utilized targeted social media strategies in conjunction with a recruitment agency to recruit adult participants aged 18–35 who could speak, read, and write in English who have the presence of at least 16 natural teeth with at least 2 abutting teeth in each sextant. This age group was selected as individuals older than age 35 may be more likely to have used other tobacco products throughout the course of their lifetime, increasing the difficulty of elucidating the specific contribution of ENDS usage to disease endpoints. In addition, participants were excluded if were currently using a nicotine patch, had active substance abuse, are currently using tobacco products, were pregnant or lactating, had a history of diabetes, HIV infection, or were currently prescribed immunosuppressant medications or antibiotics or if another household member was enrolled in the study. Eligible individuals provided informed consent and were scheduled for in-person visits with the study team.

A total of 19 participants (nine never established ENDS users and ten established ENDS users) were consented and enrolled in the study. Never established ENDS users were defined as individuals who have used less than 100 tobacco products in their lifetime. Survey results collected in our study, show the most recent use of ENDS products was one year prior to the study for two participants with the remaining never established ENDS users never having used ENDS products in their lifetime. Established ENDS users were defined as individuals who have not used combustible or any other form of tobacco in the past 90 days and exclusively used ENDS daily. These groups are defined based on current CDC definitions and were used in previous investigations[28]. Recent evidence indicates cessation of conventional tobacco use, results in reduced inflammation within 30 days[29]. Groups were composed of equal numbers of men and women and participants were not included/excluded based on socioeconomic status, race, or poverty status. The overall study design is illustrated in Fig. 1 and demographic details of participants is shown in Table 1. Upon their visit, saliva samples were collected, puffing topography assessments were completed, and exhaled emission characterization were assessed as described further below.

Puffing topography assessment

The Clinical Research Support System (CReSS; Pocket; Borgwaldt-KC, Richmond, VA) device was used to collect real-time puffing topography metrics, including puff volume (mL/puff), flow rate (mL/s), peak flow (mL/puff), inter-puff interval (s), puff duration (s), and time of peak (s) for each ENDS user[30,31]. For completion of the puffing topography assessment, each participant's own ENDS device was attached to the CReSS Pocket via a universal device adaptor and participants were instructed to take 10 puffs from their own device as they normally would. Collected real-time puffing topography information was utilized to establish puffing topography profiles for each participant and these parameters were further applied to produce firsthand exposure scenarios from their purchased device via the EAGS platform as described below (IES Technologies, Morgantown, WV)[10].

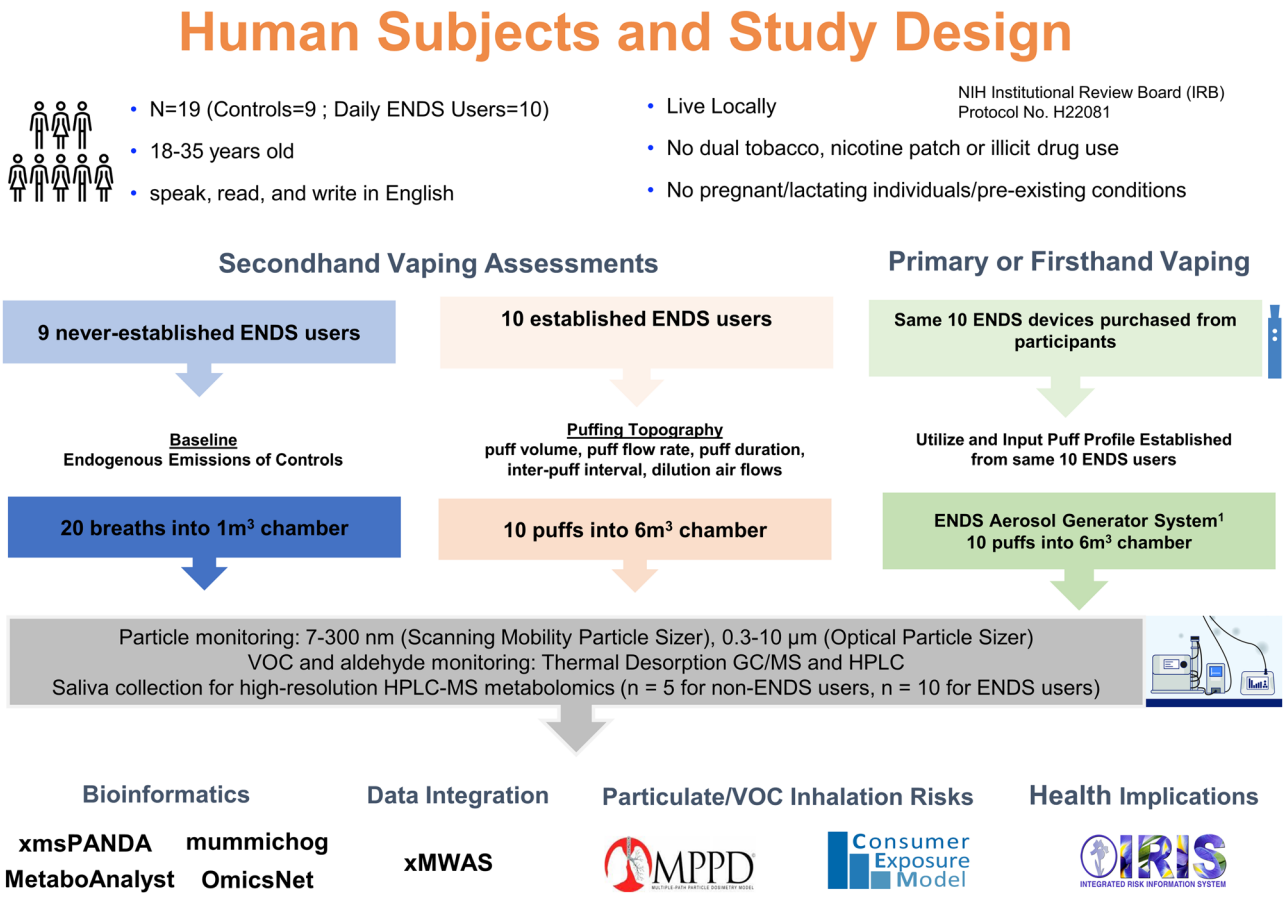

Figure 1. Illustration for study design.

	All participants	Never established ENDS users	Established ENDS user
Age	26.7 ± 3.9	25.4 ± 3.4	27.5 ± 4.4
Biological sex (n)			
Male	3	3	5
Female	6	6	5

Table 1. Average age and sex of never established and established ENDS users.

ENDS aerosol emission and exposure assessments

To investigate differential levels of ENDS aerosol exposure in real-life scenarios, three distinct exposure scenarios (baseline, firsthand, and secondhand) were employed. Baseline, firsthand, and secondhand exposure scenarios were evaluated by characterizing the emissions from never established ENDS users (n = 9), device emissions (n = 10), and established ENDS users (n = 10), respectively. In the baseline scenario, never established ENDS users generated 20 breaths into a 1 m^3 stainless steel environmental exposure chamber. In the secondhand exposure scenario, ENDS users inhaled the aerosol generated by their personal ENDS devices attached to a CReSS Pocket device, as described above, and exhaled emissions via a sterile mouthpiece into a 6m^3 chamber, providing a total of 10 puffs for analysis. To determine device emissions, personal ENDS devices from each user were purchased and utilized to generate firsthand emission. ENDS user puffing topography profiles, were applied to the EAGS platform[10], controlled by the IES software (IES Technologies, Morgantown, WV) allowing for the production of firsthand emissions from the users device which match their individual distinct puffing profile. Detailed information of the parameters and puffing topography variables applied to the EAGS platform, as previously described[10], and a description of the devices used to generate firsthand emissions are detailed in Table 2. The emissions from each scenario were characterized for particulates and VOC, with normalization based on the number of puffs for further analysis. All participant experiments were conducted with the environmental exposure chamber at static state with a minimal air exchange rate and supply air flow was applied only to compensate sampling air flow. Details of the environmental exposure chamber and measurement setup were previously published[9,10].

	Puff volume groups		
	Low (n = 3)	Medium (n = 4)	High (n = 3)
Puffing topography assessment variables			
Puff volume (mL/puff)	77.5 ± 9.08	113 ± 10.2	237 ± 53.4†*
Flow rate (mL/puff)	38.9 ± 7.58	40.9 ± 9.23	52.9 ± 8.21
Peak flow (mL/puff)	53.8 ± 10.3	57.1 ± 11.3	69.1 ± 10.2
Inter-puff interval (s)	22.1 ± 10.9	14.3 ± 2.66	62.8 ± 33.9
Puff duration (s)	2.23 ± 0.27	3.12 ± 0.44	4.44 ± 0.48*
Time of peak (s)	0.92 ± 0.32	1.3 ± 0.31	1.7 ± 0.24
ENDS device types			
Pod (n)	2	2	1
Disposable (n)	1	2	0
Pod Mod (n)	0	0	2

Table 2. Averaged puffing topography profiles and device details of low, medium, and high puff volume groups. Values are presented as means ± SE. †Statistically different compared to low. *Statistically different compared to medium; $p < 0.05$.

Particle monitoring

Particle sizes and concentrations present in generated aerosols were monitored for each scenario (e.g., baseline, firsthand, secondhand) by using the Scanning Mobility Particle Sizer (SMPS; models TSI 3080 and 3786, TSI Inc., Shoreview, MN) for 7–300 nm sized particles and Optical Particle Sizer (OPS; TSI 3330, TSI Inc., Shoreview, MN) for 0.3–10 µm sized particles. Considering the short time duration of the aerosol generation process, time resolution of the measurements for both pieces of equipment was set at 1 min. Total particle count, total mass, and geometric mean diameter (GMD) of the emitted aerosol were monitored and calculated for each scenario. For the particle size distribution analysis, data from SMPS and OPS has been merged to obtain entire particle count distribution (dN/d log Dp).

Inhalation dosimetry: particle deposition

The multiple-path particle dosimetry (MPPD; version 3.04, Applied Research Associates Inc., Albuquerque, NM) was used to determine potential particle inhalation risks and particle deposition estimates. For the analysis, the Stochastic model was selected to mimic real-life ENDS usage and exposure with input parameters as follows: constant exposure with oral breathing scenario; breathing frequency 12 per minute; tidal volume 625 mL; exposure time duration set at 6 h per day, 7 days per week for 52 weeks. Particle emission data collected from each scenario and participant, including count mean diameter, geometric standard deviation, and mass concentration (mg/m^3) were also utilized as inputs to determine the average deposited dose within the airways. Based on particle emission information inputted in the system, the average deposited dose was calculated and compared between each exposure scenario (firsthand and secondhand) and individual puff volume-based groups (e.g., low, medium, high) as further detailed in the results.

Volatile organic compound (VOC) emission analysis

For each of the exposure scenarios, generated emissions within the exposure chamber were collected on Tenax ® TA (300 mg) 60/80 mesh sorbent tube and DNPH cartridge for VOC and aldehyde analysis, respectively. Both VOC and aldehyde samples were collected for 60 min at controlled flow rates of 0.2 LPM and 0.5 LPM, respectively, by using mass flow controllers (MFC; Alicat Scientific, Tucson, Arizona). Collected VOC and aldehyde samples were analyzed with thermal desorption gas chromatography/mass spectrometry (TD-GC/MS) and high-performance liquid chromatography (HPLC) at an ISO/IEC 17025 accredited indoor air quality laboratory[32]. The data collected from the TD-GC/MS were evaluated to ensure meeting the guidelines set for identification for the limit of quantification (LOQ).

HPLC–MS based salivary metabolomics

Participants were instructed to refrain from consumption of food and liquids (aside from water) for 3 h prior to their visit. Upon arrival to the facility, participants were asked to rinse their mouth with water and after 10 min and to provide a saliva sample via passive drool technique. A total of 2 mL of saliva was collected from each participant and stored in labeled sterile cryovials with the addition of Halt™ Protease and Phosphatase Inhibitor cocktail (1% v/v, ThermoScientific, Waltham, MA) and stored at − 80 °C for downstream untargeted high-resolution HPLC–MS metabolic analysis as previously described[33–36]. To process for metabolic profiling, 750 µL of cold methanol was added to 300 µL of saliva. Samples were and centrifuged at 16,000×*g* for 8 min followed by collection of supernatants. Vacuum concentrated and dried fractions of saliva samples were reconstituted in 60 µL of HPLC diluent (95% water, 5% acetonitrile, 0.1% formic acid) followed by sonication for 5 min and centrifugation at 16,000×*g* for 8 min. The supernatants were then randomly transferred to a HPLC autosampler vial and run at one time. Separations were performed on an Agilent 1290 system (Palo Alto, CA), with a mobile phase flow rate of 0.45 mL/min. The metabolites were assayed using a Waters HSS T3 column

(1.8 µm, 2.1 × 100 mm), where the mobile phases were A (0.1% formic acid in ddiH_2O) and B (0.1% formic acid in acetonitrile). The calculated relative standard deviation for retention time was 0.27%; for area 8.4%, and for height 10.9%, all within the accepted maximum tolerance of relative standard deviation of 30% for metabolomic studies using mass spectrometry[37]. Detailed instrumentation information is described in supplemental material. These metabolite alterations were previously assessed in a separate companion study to evaluate ENDS-induced oral health effects. In our current study these metabolite alterations have been reanalyzed via a distinct bioinformatic approach (described below) to examine exposure and inhalation effects associated with ENDS usage.

Bioinformatics analysis

Peak deconvolution, integration, and statistical analysis were performed within MS-DIAL (version 4.7)[38,39]. Peak annotations were performed either using the MSP metabolomics MS/MS library, based on authentic standards (version 16) [http://prime.psc.riken.jp/compms/msdial/main.html#MSP] or made against Kyoto Encyclopedia of Genes and Genomes and the Human Metabolome Database, with the presence of primary ion enforced. Mass tolerances were 0.005 Da for MS1 and 0.01 Da for MS2 or 10 ppm maximum tolerance in *mz*. During alignment, a peak had to be present in at least 60% of at least one sample group and with a height greater than 5× of the corresponding peak in the blanks to be retained. xmsPANDA (https://github.com/kuppal2/xmsPANDA) was used for feature selection based on *p* values calculated using one-way ANOVA (*limma*) and linear regression model (*lmreg*) based on puff volume. Significant features with $p < 0.05$ from one-way ANOVA and linear regression model were then selected for one-way hierarchical cluster analysis (HCA) based on Pearson's correlation coefficient as distance metric and Ward´s linkage was used as the method to create HCA. Partial least squares-discriminant analysis (PLS-DA) was also performed using MetaboAnalyst[40]. Significant metabolic features (*limma* $p < 0.05$ and *lmreg* $p < 0.05$) were selected for metabolic pathway enrichment analysis using mummichog 2.6.0[41,42]. This statistical approach has been utilized in previous evaluations employing untargeted metabolomics[42–48].

Biomarker and metabolite-disease analysis

Annotated significant metabolic features (*limma* $p < 0.05$ and *lmreg* $p < 0.05$) were subject to univariate and multivariate receiver operating characteristic (ROC) analysis using MetaboAnalyst[40]. Metabolic features were first normalized by median, log_{10}-transformed, and auto scaled. Monte-Carlo cross validation (MCCV) with balanced sub-sampling was employed to generate ROC curves. Area under ROC curve (AUROC), T-statistics with false discovery rate (FDR), and Log_2 fold change (FC) were calculated. Linear support vector machine (SVM) was used for model classification and feature ranking. By default, two-thirds of the participants were used for feature selection and model evaluation, and the remaining were used for model validation and feature selection. Subjects were assigned to either never established ENDS user or ENDS user group for model testing and validation. Selected features were also used to reconstruct a genome-scale metabolic network using OmicsNet 2.0[49]. Recon3D database was used for metabolic reconstruction[50].

Integrative network analysis

Top ten VOCs commonly shared by firsthand and secondhand emissions with at least 70% non-missing values were selected for further analyses. To further investigate the metabolic association across different data domains, network analyses were performed for saliva metabolome, selected VOCs, particulate matter, and puff topography (puff volume) from the same exhaled or device samples (n = 10) using xMWAS based on the partial least-squares (PLS) regression method[51]. Correlation threshold was set at $|r| > 0.64$ and $p < 0.05$ for community detection. Network was visualized using Cytoscape (version 3.9.1) with Perfuse Force OpenCL layout. Metabolic features identified from network analysis were further used for pathway enrichment analysis using mummichog 2.6.0[41,42].

Inhalation risk characterization

Consumer Exposure Model (CEM) developed by the U.S. EPA was employed to calculate the risk assessment from the Acute Dose Rate (ADR), Chronic Dose Rate (CDR), and Lifetime Average Daily Dose (LADD) for both firsthand and secondhand exposure scenarios[52]. The ADR is observed to be exposure where the inhalation rate for the individual occurs during short-term exposure, 24 h/day, scenarios while the CDR uses an inhalation rate based on continued long-term exposure, 24 h/day/year, scenarios[52]. Based on the finding from a recent literature, an average daily puff number used by ENDS user was inputted as 132 puffs in this analysis[53]. Furthermore, the risk calculation for firsthand utilized near-field exposure zone information[52], to obtain an accurate estimation of the dosage that an active ENDS user is experiencing when using the device. Top ten VOCs with at least 70% non-missing values were selected to calculate the ADR and the CDR for both firsthand and secondhand exposure scenarios. The risk assessment was performed for several age groups (adult, youth, child and infant) represented by the average body weight and inhalation rates for each group[52]. The room size and airflow exchange rate were set to 50 m^3 and 0.45 (per hour), respectively, based on environmental parameters from the CEM[52]. Cancer risk (CR) was calculated for formaldehyde and acetaldehyde using $CR = LADD \times SF$ (Eq. 1), where SF is the slope factor obtained from U.S. EPA's Integrated Risk Information System (IRIS). SF for formaldehyde and acetaldehyde is 0.0455 $(mg/kg\ bw/d)^{-1}$ and 0.0077 $(mg/kg\ bw/d)^{-1}$, respectively. CEM parameters inputted for near-field far-field model in firsthand scenario risk assessment is listed in Table S1.

Statistical analysis

All the exposure scenarios include at least three replicates throughout the study. A principal component analysis (PCA) was carried out for all puffing topography profiles of ENDS users to determine the variable most representative of exposure. The results of which suggest puff volume as the mediating factor, as described

in further detail below. A paired t-test was performed to compare participle emissions and deposition results between firsthand and secondhand exposures. Further, one-way ANOVA with post-hoc testing using Fisher's LSD was performed to determine differences across puff volume groups. Sample size and replicates are noted in each figure and table, results are presented as means ± standard error with $p < 0.05$ considered statistically significant. All statistical analyses were carried out using GraphPad Prism (version 9.5.0).

Institutional review

This human subject study was approved by Advarra Institutional Review Board (IRB Protocol No. H22081).

Results

Characteristics of study participants

The general study participant characteristics (9 never established ENDS users and 10 established ENDS users) are summarized in Table 1. An approximately equal proportion of male and female participants were recruited. No significant difference between the ages of never established ENDS users and ENDS users was detected.

Puffing topography assessment

Puffing topography assessments were carried out in 10 recruited established ENDS users. To determine a potential mediator of exposure, PCA analysis was performed. Puff volume represented the highest variance and exhibited a strong correlation compared to other variables (Table S2). Based on these findings, the 10 established ENDS users were stratified into three groups based on their puff volume; low (n = 3; < 90 mL/puff), medium (n = 4; 90–150 mL/puff), and high (n = 3; > 150 mL/puff). Details of average combined puffing topography profiles for low, medium, and high puff volume groups are described in Table 2 along with comprehensive details of their devices used for firsthand and secondhand exposure scenarios. It is important to note that device format or brand, participant sex, or age were not taken into consideration in the determination of puff volume-based stratification. This stratification strategy was employed in a companion study investigating oral health effects of ENDS.

Particle monitoring

Particle concentrations and sizes were monitored for all three exposure scenarios (baseline, firsthand, and secondhand). The variations in number of particle emission, mass concentration, GMD, and particle size distribution between low (n = 3), medium (n = 4), and high (n = 3) groups from each scenario are summarized in Fig. 2. The level of particle number emission of firsthand emissions was significantly greater compared to secondhand ($p < 0.01$) and minimal levels were present in baseline emissions ($p < 0.0001$) (Table S3). Moreover, an increasing trend in number emission was noted across low, medium, and high groups in both firsthand and secondhand scenarios, although significance was only noted within firsthand groups (Fig. 2A). Likewise, increased level of mass concentration was also noted in the medium and high puff volume groups compared to the low puff volume group (Fig. 2B). Furthermore, a significant particle size reduction between firsthand and secondhand emissions was noted, especially in low ($p < 0.05$) and medium ($p < 0.01$) groups (Fig. 2C), although no significance was noted between firsthand and secondhand particle sizes in the high group (Fig. 2C).

The particle distribution of firsthand and secondhand scenarios was compared based on their puff volume (Fig. 2D–F). In the low group comparison, firsthand showed its highest peak at 79.86 nm, while secondhand showed its two peaks at 20.35 and 36.19 nm (Fig. 2D). Both firsthand and secondhand in the low group were positively skewed towards more fine particles according to SMPS data, while OPS data showed a peak in firsthand at 375 nm (Fig. 2D). Similarly, in the medium group comparison, firsthand showed its major peak at 65.52 nm, second peak at 186.01 nm with the highest peak at 550 nm (Fig. 2E). Unlike the secondhand low group, secondhand medium group showed its highest peak at 42.55 nm with the second highest peak at 116.52 nm (Fig. 2E). Within the high puff volume group comparison, firsthand also showed a bimodal distribution with one peak at 71.69 nm and another at 375 nm (Fig. 2F). Unlike other puff volume groups, in the high group comparison, particles emitted from secondhand only showed a single highest peak at 38.89 nm (Fig. 2F).

Overall, an increased level of number and mass emission was noted as the puff volume increased (Fig. 2A–F). Across different puff volume-based groups in both firsthand and secondhand, the bimodal size distribution was noted with a positively skewed trend toward more ultrafine particles (Fig. 2D–F). In particular, the particles ranging from 10 to 100 nm showed an increased level of particle number concentrations in higher puff volume groups (medium and high) compared to the low group, suggesting an increased level of PM exposure with greater puff volume (Fig. 2D–F). Additionally, OPS data consistently showed the highest peak in firsthand vape in the range from 300 to 600 nm, which could be an artifact due to the water content of the aerosols increasing light scattering (Fig. 2D–F). Furthermore, firsthand showed a slight shift towards bigger-sized particles with greater puff volume, while secondhand remained within the range between 10 and 100 nm size (Fig. 2D–F).

Inhalation dosimetry analysis: respiratory deposition

The MPPD-calculated inhalation dosimetry results (total deposited mass, total deposited surface area, total deposited dose, deposition fraction) of firsthand and secondhand are summarized in Fig. 2G–L and Table S4. Overall, increased levels of total deposited mass and surface area were noted in firsthand compared to secondhand, while both groups showed an increase with greater puff volume (Fig. 2G,H). However, the difference between firsthand and secondhand was not significant in any of puff volume-based groups (Fig. 2G,H). Likewise, the MPPD-calculated deposited dose was also higher in firsthand compared to secondhand, especially for the low ($p < 0.05$) and medium ($p < 0.01$) groups, showing an increase with greater puff volume (Fig. 2I). However, a greater total deposition fraction was noted in secondhand than firsthand across all puff volume-based groups with the significance noted for medium ($p < 0.0001$) and high groups (Fig. 2J–L). Specifically, tracheobronchial

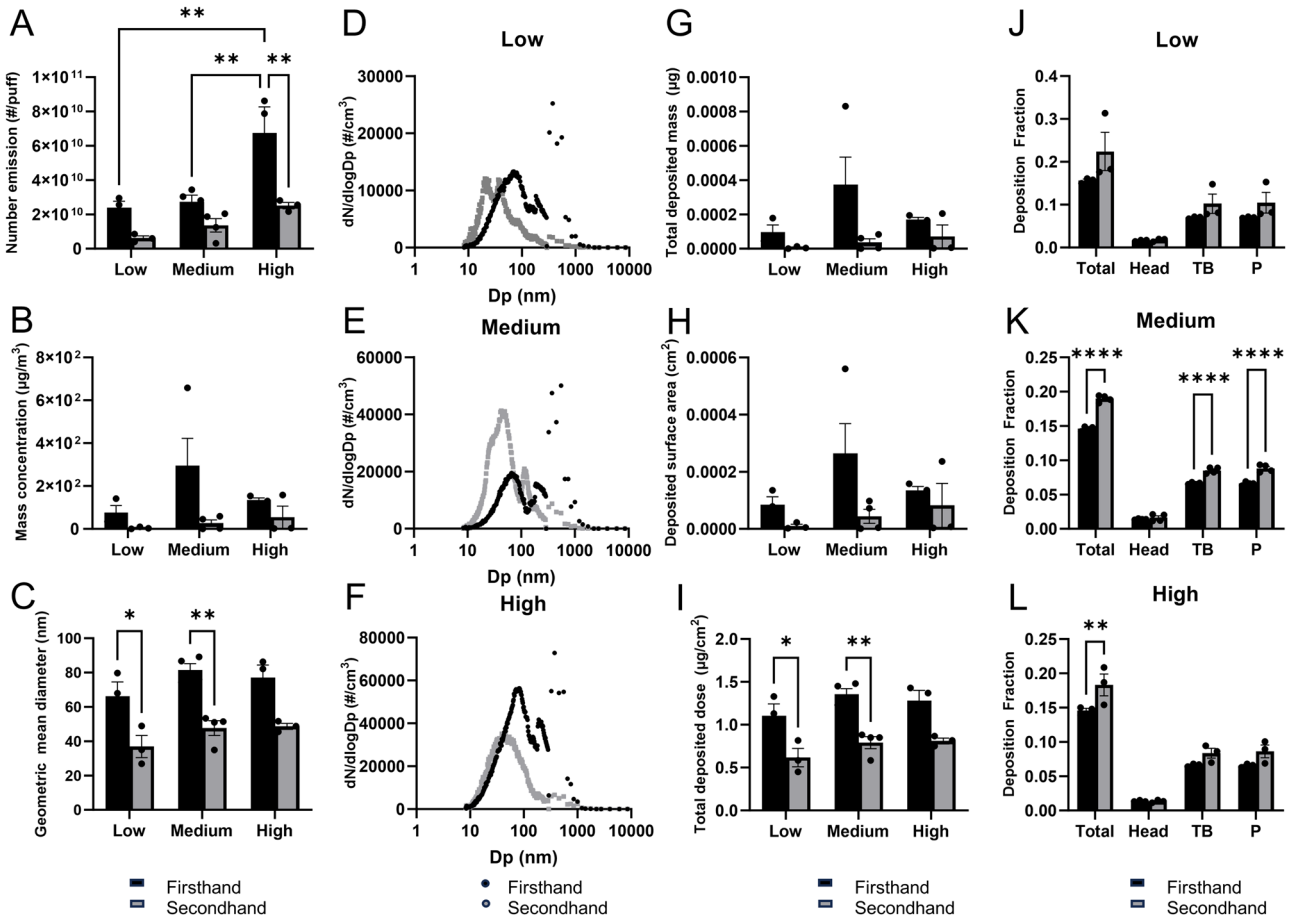

Figure 2. Differential level of particulate matter exposure and MPPD-calculated respiratory deposition in firsthand and secondhand exposure scenarios based on number emission (**A**), mass concentration (**B**), geometric mean diameter (**C**), and particle size distribution (**D–F**). Each colored bar in (**A–C**) represents an averaged value of firsthand (n = 10; black) and secondhand (n = 10; grey) with error bars representing standard errors. An upper value of each gap in y-axis represents an averaged value of baseline (n = 9). MPPD-calculated respiratory deposition of firsthand (n = 10) and secondhand (n = 10) exposure scenarios are shown in (**G–L**). Scenario and puff volume-based comparison has demonstrated an averaged total deposited mass (**G**), deposited surface area (**H**), and an estimated inhaled dose (**I**), and deposition fraction (**J–L**). Each bar represents averaged values from each group with an error bar representing standard error; firsthand exposure scenario (black), secondhand exposure scenario (grey). Colored bars (**A–C,G–L**)/dots (**D–F**) represent an averaged values of low (n = 3), medium (n = 4), and high (n = 3) groups from firsthand (black) and secondhand (grey) scenarios. Significance was determined by two-sided $p < 0.05$ in ANOVA analysis, followed by Bonferroni's multiple comparison test. For averages and standard errors of each scenario, see Table S3. ns $p > 0.05$, $^{*}p < 0.05$, $^{**}p < 0.01$, $^{***}p < 0.001$, $^{****}p < 0.0001$. Detailed values for baseline, firsthand, and secondhand can be found in Table S4. Head: head airway. *TB* tracheobronchial, *P* pulmonary alveoli. Low: puff volumes < 90 mL/puff; Medium: 90 mL/puff < puff volumes < 150 mL/puff; High: puff volumes > 150 mL/puff.

(TB) and pulmonary alveoli (P) regions showed a greater deposition fraction compared to head region in all puff volume-based groups. In particular, secondhand medium group showed significantly higher regional deposition fraction in TB ($p < 0.0001$) and P ($p < 0.0001$) compared to firsthand medium group (Fig. 2K).

VOC emissions

The firsthand and secondhand emissions were cross-referenced to identify the common VOCs between both cases. The top 20 VOC emissions were collected by identifying the VOCs that are commonly shared by user exhalation and device emission and have at least 30% non-missing values (Table 3, see associated physicochemical properties in Tables S5, S6). The top 20 VOCs have been observed as chemical components of the e-liquids or by-products from their decomposition and consumption from the vaporization process of the devices. In general, the concentration of VOCs from firsthand emission increases as the puff volume increases, especially in 1,2-propanediol, hexanal, nonanal, and toluene (Fig. S7), while secondhand showed an increase in decanal, formaldehyde, 3-piperidinol, 1-ethyl-, 1,2-propanediol, and acetaldehyde (Fig. S6). The secondhand emissions are much less than the firsthand emissions for almost all the VOCs, except for a few bio-active VOCs (Table 3).

CASRN	CID	Firsthand emission (μg/puff)					Secondhand emission (μg/puff)				
		Low	Med	High	Overall	Detection freq. (%)	Low	Med	High	Overall	Detection freq. (%)
50-00-0	Formaldehyde	14.98 ± 12.96	0.81 ± 0.43	1.22 ± 0.17	5.18 ± 3.97	100	1.52 ± 0.67	2.04 ± 0.11	1.85 ± 0.2	1.83 ± 0.2	100
57-55-6	1,2-Propanediol (propylene glycol)	474.88 ± 67.78	1015.53 ± 293.37	1864.76 ± 343.45	1108.1 ± 229.08	100	41.49 ± 22.46	47.52 ± 38.19	46 ± 41.13	45.26 ± 18.48	90
111-71-7	Heptanal (heptaldehyde)	0.24 ± 0.06	0.22 ± 0.03	0.45 ± 0.17	0.3 ± 0.06	100	0.3 ± 0.16	0.21 ± 0.08	0.34 ± 0.12	0.27 ± 0.06	80
75-07-0	Acetaldehyde	5.26 ± 4.24	1.35 ± 0.55	0.9 ± 0.27	2.39 ± 1.28	90	1.06 ± 0.48	0.71 ± 0.33	1.43 ± 0.5	1.03 ± 0.24	90
112-31-2	Decanal	0.19 ± 0.1	0.53 ± 0.15	0.68 ± 0.34	0.47 ± 0.12	90	0.17 ± 0.12	0.17 ± 0	0.59 ± 0.29	0.29 ± 0.1	90
13444-24-1	3-Piperidinol, 1-ethyl-	4.07 ± 3.91	21.22 ± 13.64	7.7 ± 2.06	12.02 ± 5.71	90	0.01 ± 0.01	0.55 ± 0.19	0.55 ± 0.04	0.39 ± 0.11	80
124-19-6	Nonyl aldehyde (nonanal)	0.48 ± 0.24	0.64 ± 0.25	1.17 ± 0.23	0.75 ± 0.16	80	0.57 ± 0.29	0.22 ± 0.1	1.18 ± 0.49	0.61 ± 0.2	80
54-11-5	Pyridine, 3-(1-methyl-2-pyrrolidinyl)-, (S)-(nicotine)	0.42 ± 0.38	2.75 ± 2.26	10.25 ± 2.36	4.3 ± 1.69	80	0.11 ± 0.11	0.08 ± 0.08	0.17 ± 0.17	0.12 ± 0.06	40
6846-50-0	TXIB (2,2,4-trimethyl-1,3-pentanediol diisobutyrate)	0.04 ± 0.04	0.08 ± 0.01	0.09 ± 0.03	0.07 ± 0.02	80	0.02 ± 0.02	0.01 ± 0.01	0.15 ± 0.06	0.06 ± 0.03	60
66-25-1	Hexanal	0.24 ± 0.06	0.21 ± 0.13	1.12 ± 0.38	0.49 ± 0.18	80	0.52 ± 0.29	0.31 ± 0.11	0.62 ± 0.22	0.47 ± 0.11	80
108-88-3	Toluene (methylbenzene)	0.14 ± 0.1	0.14 ± 0.11	0.91 ± 0.45	0.37 ± 0.17	70	0.32 ± 0.16	0.37 ± 0.17	0.23 ± 0.08	0.31 ± 0.08	80
1330-20-7	Xylenes (total)	0.19 ± 0.07	0.05 ± 0.05	0.18 ± 0.03	0.13 ± 0.03	70	0.15 ± 0.08	0.27 ± 0.13	0.17 ± 0.08	0.2 ± 0.06	70
102-76-1	1,2,3-Propanetriol, triacetate (triacetin)	0.32 ± 0.26	1.27 ± 1.01	0.76 ± 0.41	0.83 ± 0.41	70	0.08 ± 0.08	0.08 ± 0.05	0.16 ± 0.05	0.11 ± 0.03	60
80-56-8	Pinene, alpha (2,6,6-trimethyl-bicyclo[3.1.1]hept-2-ene)	0.06 ± 0.05	0.03 ± 0.03	0.04 ± 0.02	0.04 ± 0.02	50	0.14 ± 0.14	0.27 ± 0.12	0.19 ± 0.04	0.21 ± 0.06	70
71-36-3	1-Butanol (*N*-butyl alcohol)	0.25 ± 0.13	0.15 ± 0.09	0.6 ± 0.6	0.32 ± 0.18	50	0.63 ± 0.32	0.21 ± 0.11	0.84 ± 0.34	0.53 ± 0.15	80
100-42-5	Styrene	0.11 ± 0.06	0 ± 0	0.18 ± 0.08	0.09 ± 0.04	50	0.2 ± 0.11	0.22 ± 0.07	0.17 ± 0.05	0.2 ± 0.04	80
64-17-5	Ethanol	0 ± 0	18.71 ± 8	4.35 ± 4.35	8.79 ± 4.17	40	10.87 ± 5.91	19.07 ± 9.05	44.17 ± 20.06	24.14 ± 7.78	80
104-76-7	1-Hexanol, 2-ethyl	0.39 ± 0.26	0.33 ± 0.22	0 ± 0	0.25 ± 0.12	50	0.52 ± 0.3	0.44 ± 0.15	0.62 ± 0.07	0.52 ± 0.1	80
629-59-4	Tetradecane	0.11 ± 0.06	0.03 ± 0.02	0 ± 0	0.05 ± 0.02	40	0.1 ± 0.05	0.09 ± 0.05	0.1 ± 0.06	0.1 ± 0.03	80
124-13-0	Octanal	0.87 ± 0.6	0.15 ± 0.15	0 ± 0	0.32 ± 0.2	40	0.54 ± 0.28	0.3 ± 0.11	0.89 ± 0.18	0.55 ± 0.12	80

Table 3. Firsthand and secondhand VOC exposure level. Low: puff volumes < 90 mL/puff; Medium: 90 mL/puff < puff volumes < 150 mL/puff; High: puff volumes > 150 mL/puff.

Vaping behavior associated salivary metabolic responses

Over 50,000 metabolic features were yielded from Agilent 6545 Q-TOF mass spectrometer with positive ionization mode after data filtering using xmsPANDA. One-way ANOVA using *limma* showed 10,095 features were significantly altered ($p < 0.05$, Fig. 3A). Additionally, linear regression analysis using *lmreg* revealed 2096 significant features ($p < 0.05$, Fig. 3B), with 1160 positively associated and 916 negatively associated. A total of 263 metabolic features were finally selected by identifying the overlapping features from *limma* and *lmreg* analyses. One-way HCA of 263 metabolic features selected from one-way ANOVA and linear regression analyses clearly showed two clusters, with 53 metabolites in cluster I (negative association) and 210 metabolites in cluster II (positive association), as shown in Fig. 3C. PLS-DA of selected metabolic features showed a clear separation between ENDS users and never established ENDS users, as well as a noted trajectory from low to high puff volumes among ENDS users (Fig. 3D). Together with the one-way HCA shown in Fig. 3C, PLS-DA demonstrated the vaping behavioral response was largely driven by ENDS participants with a high puff volume. Pathway enrichment analysis was carried out using *mummichog* for the 263 selected metabolic features. 263 significant features were putatively mapped to 15 unique empirical compounds, resulting perturbation in major metabolic pathways include energy metabolisms [pyruvate ($p = 2 \times 10^{-5}$), glycolysis and gluconeogenesis ($p = 0.01$)], amino acids [glycine, serine, alanine and threonine metabolism ($p = 0.0075$), β-alanine metabolism ($p = 0.024$)], and lipid regulation [carnitine shuttle ($p = 0.014$), propanoate metabolism ($p = 0.019$), prostaglandin formation ($p = 0.041$), glycerophospholipid metabolism ($p = 0.047$)], as shown in Fig. 3E. Noticeably, mean saliva levels of L-palmitoylcarnitine (Fig. 3F), lactate (Fig. 3G), methylglyoxal (Fig. 3H), and 6-hydroxyhexnaoate (Fig. 3I), were significantly lower than never established ENDS users, while leukotriene D4 (Fig. 3J) and 3-hydroxyquinine (Fig. 3K) had higher mean levels in ENDS users with an increasing trajectory from low to high puff volumes. Other notable metabolites include butyrate (Fig. S1A), retinoate (Fig. S1B), 2′,3′-cyclic UMP (Fig. S1C), anserine

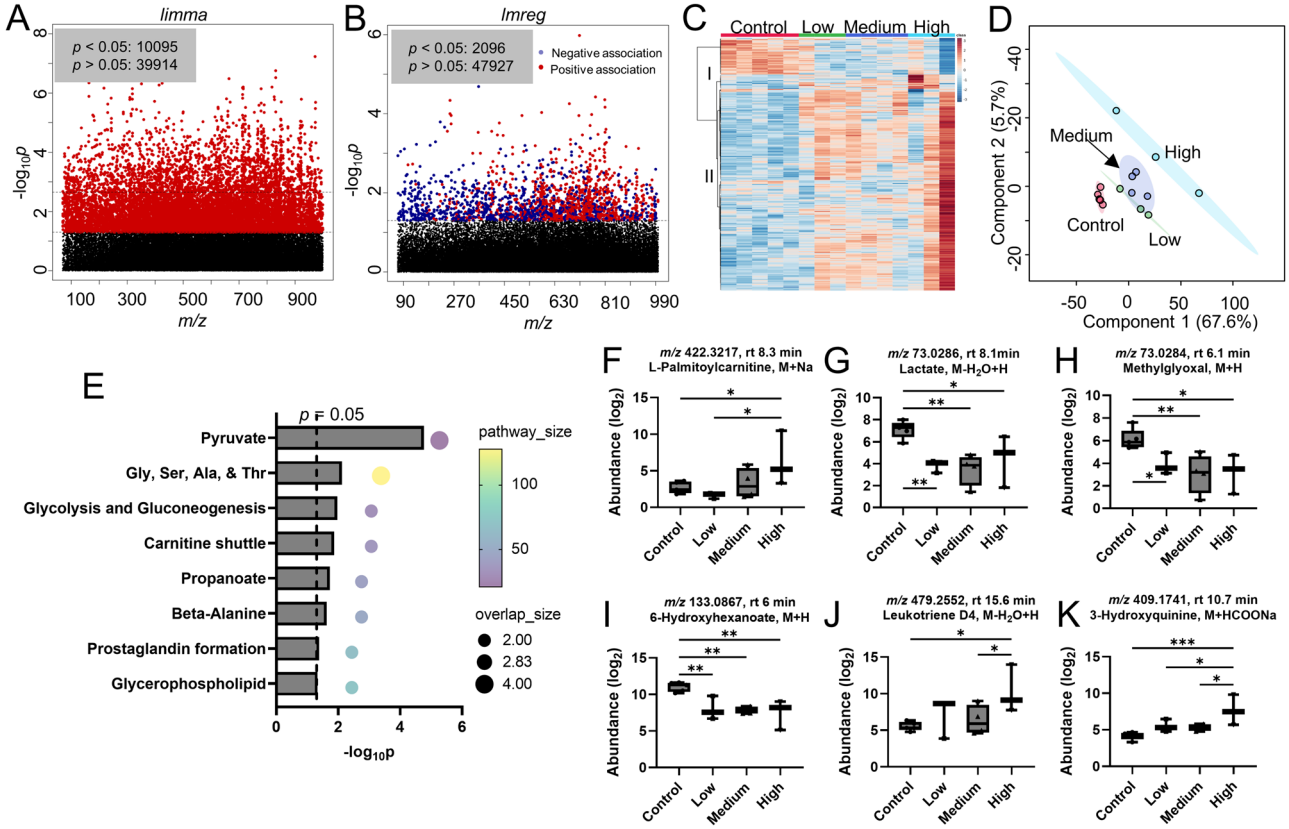

Figure 3. Metabolic perturbation induced by ENDS use with predefined vaping behavior based on puff volumes. (**A**) Manhattan plot of metabolic features showing $-\log_{10}p$ using *limma* analysis. Features with significance (10,095 features, $p < 0.05$) are shown in red. (**B**) Manhattan plot of metabolic features showing $-\log_{10}p$ using *lmreg* analysis. Features with significance (2096 features, $p < 0.05$) are shown in red (positive association) and blue (negative association). (**C**) One-way HCA using 263 metabolic features with $p < 0.05$ from (**A**,**B**). (**D**) PLS-DA plot of the selected 263 metabolic features. (**E**) Pathway enrichment analysis using the 263 metabolic features. Selected significant metabolites are individually plotted in (**F**–**K**): (**F**) butyrate, (**G**) lactate, (**H**) methylglyoxal, (**I**) leukotriene D4, (**J**) 6-hydroxyhexanoate, (**K**) 3-hydroxyquinine. One-way ANOVA with Fisher's LSD post hoc test was performed to obtain statistical significance between groups, with $^{*}p < 0.05$, and $^{**}p < 0.01$. n = 5 for controls, n = 3 for low, n = 4 for medium, n = 3 for high puff volume group. Low: puff volumes < 90 mL/puff; Medium: 90 mL/puff < puff volumes < 150 mL/puff; High: puff volumes > 150 mL/puff.

(Fig. S1D), and 4-hydroxyphenylacetaldehyde (Fig. S1E), GDP-D-mannose (Fig. S1F), pregnenolone sulfate (Fig. S1G), cholesterol sulfate (Fig. S1H), and taurolithocholate (Fig. S1I).

To evaluate the potential application of those 15 metabolic features with identified empirical compound ID as biomarker for ENDS users, we performed univariate and multivariate ROC analyses using MCCV (Table S7). Methylglyoxal, butyrate, 4-hydroxyphenylacetaldehyde, and 6-hydroxyhexanoate were the top 4 metabolites with AUROC > 0.9 and mean importance measure > 2.9 (Table S7, Fig. 4C). MCCV generated a model with two features with an AUC of 0.95 (95% CI 0.79–1) and a prediction accuracy of 84.4%. As the number of features increase, the better performance of MCCV was observed, with highest AUC of 1 (95% CI 1–1) and prediction accuracy of 91.3% when top 10 metabolic features were used for classification (Fig. 4A,B).

We next utilized the 15 metabolic features to reconstruct genome-scale metabolic network. One out of two subnetworks that had disease correlations were identified and shown in Fig. 4D. A total of 10 metabolites were associated in the identified subnetwork (Fig. 4D, Table S8), including pregnenolone sulfate, 4-hydroxyphenylacetaldehyde, methylglyoxal, butyrate, L-palmitoylcarnitine, cholesterol sulfate, leukotriene D4, taurolithocholate, retinoate, and lactate. Metabolite-disease network analysis showed several disease-related pathways following the genome-scale reconstruction (Fig. 4E). Gastric cancer and lung diseases including asthma ($p = 0.000187$), non-small cell lung cancer ($p = 0.0178$), and small cell lung cancer ($p = 0.00781$) were identified to be directly associated with the input queries of metabolites. Other disease types including sensory dysfunction, neurological diseases, endocrine and metabolic diseases, and circulatory dysfunctions were associated with the genes from the genome-scale metabolic network reconstruction.

Integrative metabolome-wide association network analysis and inhalation risks based on vaping behavior

Integrative network analysis was conducted to further investigate the potential correlation among four different datasets, including puff topography (puff volumes), particle characterization, VOCs emission, and saliva metabolome. A total of 5822 metabolic features were identified and clustered into seven clusters (Fig. 5A). Puff volume was clustered into cluster 7, with 1,2-propanediol, hexanal, nonanal, toluene from firsthand emission, and 1238 metabolic features. As shown in Fig. 5B, pathway enrichment analysis using the 1238 metabolic features from cluster 7 generated eight pathways including *N*-glycan biosynthesis ($p = 0.012$), porphyrin metabolism

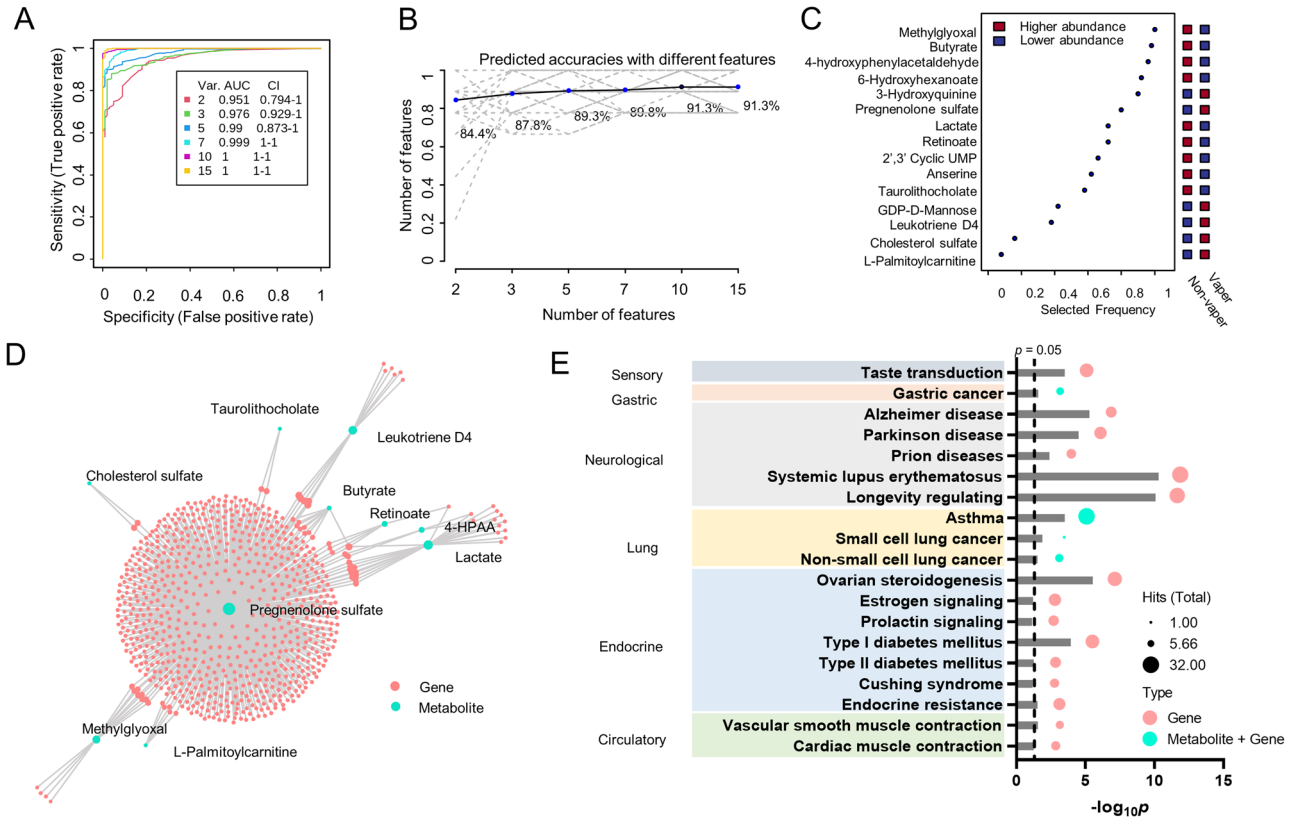

Figure 4. ROC analyses and genome-scale metabolic network reconstruction using 15 metabolic features with HMDB IDs. (**A**) Multivariant ROC analysis using MCCV. Prediction performance with different number of features is shown in (**B**). (**C**) Shows the ranked metabolites based on selected frequency. (**D**) Genome-scale metabolic network reconstruction using Recon3D database. (**E**) Metabolite-disease network analysis shows metabolic pathways associated with the reconstructed genome-scale metabolic network in (**D**). Integrative *p* values based on the hits of genes and metabolites were used for pathway selection.

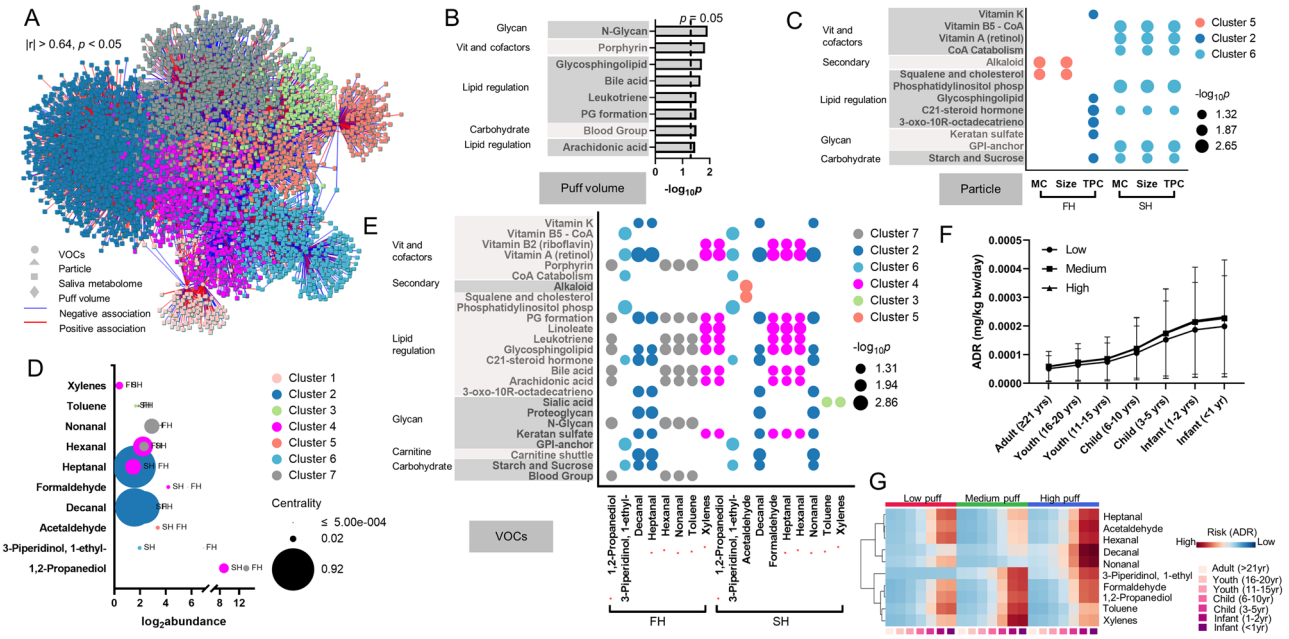

Figure 5. Four-way integrative network analysis between puff volume, particle characterization, top 10 shared VOCs, and salivary metabolome. (**A**) Visualization of network interactions, showing seven distinct clusters. Correlation threshold was set at $|r| > 0.64$, $p < 0.05$. (**B**) Pathway enrichment analysis using the metabolites from cluster 7 that had puff volume included. (**C**) Significantly perturbed pathways that were associated with particle characterization from firsthand (FH) or secondhand (SH) emission. *MC* mass concentration (μg/cm^3), *TPC* total particle counts (#/cm^3), size (nm). (**D**) Abundance and network centrality of top 10 shared VOCs from FH and SH emissions. (**E**) Pathway alteration associated with VOCs. Red asterisks indicate differential effects on pathways were observed for the same VOC between FH and SH emissions. Risk assessment with (**F**) average estimated acute dose rate (ADR, mg/kg bw/day) for 10 shared VOCs from secondhand emission. (**G**) Shows one-way HCA for the estimated ADR for secondhand emitted VOCs separated by puff groups. *PG* prostaglandins, *ADR* acute dose rate. Low: puff volumes < 90 mL/puff; Medium: 90 mL/puff < puff volumes < 150 mL/puff; High: puff volumes > 150 mL/puff.

($p = 0.015$), glycosphingolipid biosynthesis ($p = 0.02$), bile acid biosynthesis ($p = 0.022$), leukotriene metabolism ($p = 0.031$), prostaglandin formation ($p = 0.031$), blood group biosynthesis ($p = 0.031$), and arachidonic acid metabolism ($p = 0.034$). The pathways associated with particle characterization are shown in Fig. 5C. The mass concentration and size of the particle emitted from firsthand exposure were clustered into cluster 5, with the acetaldehyde from the secondhand exposure and 564 metabolic features. Pathway enrichment analysis revealed two pathways, including alkaloid biosynthesis ($p = 0.007$) and squalene and cholesterol biosynthesis ($p = 0.012$) were significantly associated. The total particle count from firsthand emission was clustered into cluster 2, with decanal and heptanal also from firsthand emission and 2082 metabolic features. A total of nine pathways, mainly focused on lipid-regulated pathways, were identified (Fig. 5C). The mass concentration, particle size, and total particle counts from secondhand emission all grouped into cluster 6, with 1-ethyl-3-piperidinol from firsthand and secondhand emission, as well as 637 metabolic features. Seven pathways, including major vitamin and cofactor metabolisms and two lipid-regulated pathways, were significantly associated with cluster 6.

The top ten VOCs shared between firsthand and secondhand emissions were distributed into all seven clusters. Toluene, decanal, nonanal, hexanal, xylenes, and heptanal had similar total abundance across firsthand and secondhand emissions (Fig. 5D). 1-Ethyl-3-piperidinol, 1,2-propanediol, acetaldehyde, decanal, formaldehyde had higher abundance in firsthand emission (Fig. 5D). Heptanal from firsthand emission had highest centrality score, followed by decanal from secondhand and firsthand emission (Fig. 5D). Pathway enrichment analysis using the metabolic features from each cluster indicate xylenes and toluene had the most differential association between firsthand and secondhand exposure (Fig. 5E). Xylenes and toluene from firsthand exposure were mainly associated with vitamins and cofactors, lipid regulation, and glycans, whereas in secondhand exposure they were only associated with sialic acid metabolism. 1,2-Propanediol, nonanal, hexanal, and heptanal had more pathway associated from secondhand emission and were in the same cluster. 1-Ethyl-3-piperidinol and decanal from firsthand and secondhand emission were in the same cluster and had the exact pathways associated. Overall, majority of the selected VOCs were associated with inflammatory response related pathways, for example, arachidonic acid, leukotriene, prostaglandins, and bile acids, metabolisms. It is noted that cluster 1 with acetaldehyde and formaldehyde from firsthand emission did not generate any significant pathways. A panel of selected metabolites were plotted against puff volumes as shown in Fig. S2 and plotted against particle characterizations and VOCs from firsthand (Fig. S3) and secondhand (Fig. S4) emissions.

Risk assessment using the CEM model revealed almost all ten selected VOCs from secondhand vaping emissions could pose significantly higher acute exposure dose (Fig. 5F,G, Tables S9, S11) and chronic exposure

dose (Fig. S5B,C, Tables S10, S12), and therefore higher health risks to younger age groups. Importantly, a puff behavior-dependent exposure risk was identified, showing increasing ADR and CDR as the puff volumes increase (Fig. 5F, Suppl Fig. S5B). Decanal (Fig. S6A,F), formaldehyde (Fig. S6B,G), 1-ethyl-3-piperidinol (Fig. S6C,H), and 1,2-propanediol (Fig. S6D,I) from secondhand emission were the major VOCs driving the puff volume-dependent pattern. Higher exposure risk was found associated with high puff volume group for acetaldehyde (Figs. S6E, S7J). Notably, we also identified a clear puff volume dependent exposure risk for several VOCs from firsthand emission (Fig. S5D–F), including 1,2-propanediol (Fig. S7A), hexanal (Fig. S7B), nonanal (Fig. S7C), and toluene (Fig. S7D), which is consistent with the puff volume dependent increase in each corresponding VOC (Fig. S7E–H). Puff volume-dependent increases in firsthand ADR and CDR were also noted in Fig. S5G,H, respectively. While the majority of VOC emission and exposure risk were decreased in secondhand exposure scenario in comparison to firsthand emission (Fig. S8), several VOCs had higher exposure and risk level in secondhand exposure. As shown in Fig. S8, further analysis revealed that formaldehyde exposure and estimated health risks were substantially increased in secondhand exposure scenario for medium (abundance increase by 2.2-fold, lifetime average daily dose increase by 2.5-fold) and high puff (abundance increase by 1.99-fold, lifetime average daily dose increase by 1.51-fold) group. Acetaldehyde exposure and estimated health risks were increased in secondhand exposure scenario for high puff group (abundance increase by 2.12-fold, lifetime average daily dose increase by 1.59-fold), whereas xylenes exposure and associated health risks were increased in secondhand exposure scenario for medium puff group (abundance increase by 3.03-fold, lifetime average daily dose increase by 4.98-fold). Toluene exposure and estimated health risks increased in secondhand exposure scenario for low and medium puff group. Based on the modeled lifetime average daily exposure levels, the cancer risk of formaldehyde from secondhand emissions showed a puff volume-dependent increase with 1.13×10^{-5} for medium puff group and 1.03×10^{-5} for high puff group, both were significantly higher than 8.51×10^{-6} from low puff volume group (Fig. S9A). The trend was opposite for formaldehyde from firsthand emission with a cancer risk of 8.37×10^{-5} for low puff group, 4.5×10^{-6} for medium puff group, and 6.83×10^{-6} for high puff volume group. Lower cancer risks were found with acetaldehyde, with highest of 4.97×10^{-6} for low puff volume group from firsthand emission and 1.35×10^{-6} for high puff group from secondhand emission (Fig. S9D). Leukotriene D4 level in saliva increased with higher formaldehyde level (Fig. S9B) and higher acetaldehyde level (Fig. S9E), though not statistically significant. In contrast, retinoate level in saliva decreased with higher formaldehyde level (Fig. S9C) and higher acetaldehyde level (Fig. S9F).

Discussion

In this study, a comprehensive investigation of potential secondhand vaping exposure risks in an indoor environment was performed based on the physical and chemical characterization of the emitted aerosols along with its impact on various metabolic processes (see schematic illustration in Fig. 6). Current studies of potential impact of secondhand vaping on indoor air quality are primarily focusing on compositional analysis of the emission, while this study is one of the few that demonstrates real-life personal exposure scenarios by conducting a comparative analysis between firsthand and secondhand with puffing topography profile-matched data[10,20,54]

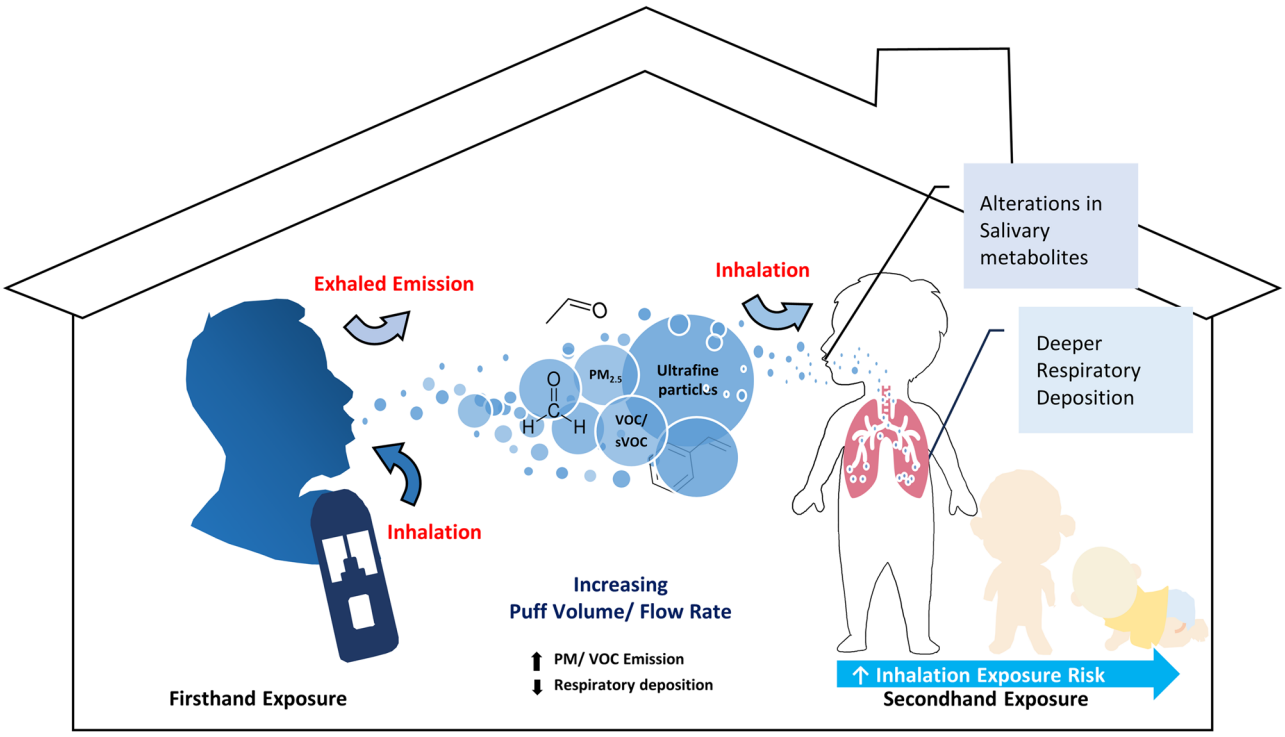

Figure 6. Illustrative summary for major outcomes.

and metabolomic outcomes associated with each exposure scenario. Moreover, the calculated vital capacity (VC) and forced vital capacity (FVC) did not show significant differences among the low, medium, and high puff volume groups (Fig. S10). The comparable lung functions across different puff volume groups ensured that puff topography profiling was directly linked to user behaviors, rather than individual lung function.

To assess the respiratory health risk of secondhand vaping, it is essential to understand the process of aerosol delivery and deposition within the human respiratory tract, which is highly dependent on aerosol particle characteristics[9,55]. Consistent with previous studies, we observed high levels of particle number and mass concentration in both firsthand and secondhand, which increased linearly with greater puff volume[56–58]. Moreover, a significant reduction in particle size was noted in secondhand compared to firsthand aerosols across all puff volume-based groups, which aligns with the range reported in other studies[55,56]. Additionally, the bimodal size distribution of particles smaller than 2.5 μm observed in this study is consistent with previous research, indicating a potential for deeper respiratory PM deposition in both firsthand and secondhand exposures[56,57]. Our particle monitoring results demonstrate that particle concentrations and size distributions are strongly influenced by vaping behavior, highlighting that the puff volume and flow rate are critical parameters that contribute to an increase in PM exposure levels.

In addition to particle monitoring findings, our particle deposition modeling results provide an estimated deposition risk by accounting for morphological and physiological factors of the respiratory system[59]. Our total deposited dose result showed a significantly higher level in firsthand compared to secondhand with a linear increase across puff volume-based groups, while the unique finding was observed in respiratory deposition fraction results. Despite the MPPD-estimated total deposited dose being smaller in secondhand, we have noted a greater deposition fraction compared to firsthand, particularly in the tracheobronchial and pulmonary alveoli regions. Moreover, our result also indicated that greater puff volume leads to higher total respiratory deposition fraction in secondhand, which could be due to a higher particle concentration of smaller particles[60,61]. This unique finding suggests that secondhand emission may pose a significant respiratory health risk, as the deposited particle increases the potential to cause adverse effects in the pulmonary regions[62,63]. However, it is important to note that a higher deposition fraction observed in secondhand does not necessarily imply a higher overall health risk compared to firsthand exposure. Factors such as the chemical composition, dilution, and bioavailability of the emitted aerosol also play a key role in determining the overall health impact.

As a non-invasive approach, saliva has been studied and used for the diagnosis and prediction of diseases, including oral diseases, diabetes, cardiovascular disease, and lung cancer among many others[64,65]. In this study, we applied untargeted high-resolution metabolomics to investigate the salivary metabolic alterations in saliva samples collected from non-vaping and vaping subjects stratified based on puff volume. This stratification method based on an individual's puff volume likely enhanced our ability to discern exposure-induced responses, which would not have been evident compiling data based on ENDS usage only. Specifically, our integrative approach by combining statistical analyses from one-way ANOVA and linear regression model revealed 15 metabolites with empirical compound IDs showing significant different levels among puff volume groups. Consistent with findings from other studies[66,67], genome-scale metabolic reconstruction suggested the metabolic perturbation induced by vaping could further contribute to a range of adverse health outcomes, including lung cancer and asthma. Retinoate and leukotriene D4 were two notable metabolites that were directly associated with lung diseases as revealed by our metabolite-disease network analysis. Retinoate, the bioactive vitamin A metabolite, is essential in regulating major cell metabolisms including carbohydrate, lipid, and protein metabolism[68], which aligns well with our findings. Moreover, retinoate plays a critical role in the formation of lung primordium and postnatal lung development[69]. Deficiency of retinoate is associated with impaired lung function[69,70] and lung diseases, including asthma[71] and cancer[72]. Our results indicate that the level of retinoate was significantly decreased in a puff volume dependent manner and was associated with small cell lung cancer and non-small cell lung cancer. Leukotriene D4 could increase collagen production[73], cause gas exchange disturbances and bronchoconstriction[74,75], and is associated with asthma[75], which is consistent with our findings. Furthermore, we also observed a clear puff volume dependent increase in leukotriene C4 (Fig. S2A) and 20-hydroxyleukotriene E4 (Fig. S2B). Leukotriene C4 can be converted to leukotriene D4 by gamma-glutamyltransferase and plays important role in the pathogenesis of lung fibrosis and asthma[76,77]. 20-Hydroxy-leukotriene E4 can be produced from the lipid oxidation of leukotriene E4, which is a metabolite of leukotriene D4. Leukotriene C4, D4, and E4 are known as cysteinyl leukotrienes as key inflammatory lipid mediators synthesized from arachidonic acid that are associated with impaired airway function and development of lung diseases[78].

Notably, our integrative metabolome-wide association network analysis indicated that puff volume was shown to be associated with major lipid-regulated pathways including glycosphingolipid biosynthesis, bile acid biosynthesis, leukotriene metabolism, prostaglandin formation, and arachidonic acid metabolism. As we have discussed above, leukotriene metabolism, prostaglandin formation, and arachidonic acid metabolism are known key players in regulating lung inflammation and disease progression. An earlier study found that increased glycine and taurine conjugated bile acids levels were associated with pulmonary arterial hypertension[79]. Indeed, we found relevant bile acids metabolites, including taurolithocholate (Fig. S2E), taurodeoxycholate (Fig. S2F), and chenodeoxycholate (Fig. S2G), were increased in a puff volume dependent manner. The increased salivary bile acids are likely to cause elevated bile acids level in lungs, which could cause lung injury[80,81]. Overall, our results suggest increasing puff volumes could potentially contribute to inflammation and lung diseases and could act as a potential health moderator that dictates the magnitude and severity of outcomes.

We also noted that PM and several VOCs emitted from ENDS use may lead to disruption in lipid homeostasis, especially steroid and hormone related pathways. Literature showed ENDS, even when nicotine-free, could release particles and VOCs that disturb the steroid and hormonal balance and affect reproductive systems[82]. Our results indicate that particles from secondhand emission had more prominent correlation with disruption in hormone pathways than that from firsthand emission, suggesting a higher health risk related to hormone

metabolisms may be linked to secondhand emission and likely due to our estimated higher respiratory deposition fraction in secondhand exposure. Moreover, although the selected ten VOCs shared between firsthand and secondhand emissions were distributed into all seven clusters, there is considerable metabolic overlap between firsthand and secondhand emissions. Importantly, 1,2-propanediol, hexanal, nonanal, and toluene from firsthand and secondhand emission were associated with metabolites from the same cluster with puff volume, therefore had same metabolic pathway outcome. 1,2-Propanediol generally constitutes approximately 60% of the e-liquid as carrier solvent[83]. Although 1,2-propanediol is categorized GRAS (generally recognized as safe) by the U.S. FDA, accumulating evidence show that vaporized 1,2-propanediol has been reportedly tied to increased upper respiratory irritation[84] and elevated risk of asthma[85], disrupting normal lung function. A recent study showed that 1,2-propanediol could cause lipid oxidation and DNA damage in HAECs, disrupt lipid homeostasis in alveolar macrophages and epithelial cells, downregulate innate immunity, leading to lung inflammation and tissue damage[86]. Hexanal is commonly used as flavoring reagent to produce fruity flavors in flavor industry and is commonly found in e-liquids[87]. Exposure to hexanal could cause elevated IL-8 in primary bronchial epithelial cells at ALI[88], elevated levels of IL-1β, IL-8, and TNF-α in naïve THP-1 cells[87]. Nonanal is known to be toxic and has been detected in ENDS emission[87,89,90]. Earlier studies showed that nonanal was associated with several lung diseases[91], including acute respiratory distress syndrome[92]. Toluene has also been found in the ENDS vapor[15,93]. Exposure to toluene is known to cause irritation of the upper respiratory tract and central nervous system dysfunction. The association of these four VOCs from both firsthand and secondhand vaping emission with puff volume and related metabolic pathways indicates, once again, that vaping behavior such as puff volume could be a regulating factor to the health risks associated with vaping.

Moreover, our risk assessment using CEM model showed that several VOCs from secondhand emission exhibited increased health risks in a puff volume and age-dependent manner, including decanal, formaldehyde, 1-ethyl-3-piperidinol, 1,2-propanediol, and acetaldehyde. While 1,2-propanediol, formaldehyde, and acetaldehyde were the top three VOCs accounted for over 95% of the overall VOC emission and exposure risk, only formaldehyde and acetaldehyde are IARC Group 1 or 2 carcinogens that are commonly found in ENDS aerosols[94]. Cancer risks for formaldehyde and acetaldehyde from secondhand exposure increased as puff volume increases, a trending pattern that was opposite from firsthand exposure. It is noted that cancer risks for formaldehyde from secondhand emissions at medium and high puff groups were over 10× higher than those recommended by U.S. EPA (1×10^{-6}), whereas acetaldehyde only had slightly higher cancer risk (1.35×10^{-6}) at high puff group from secondhand emission. This is highly consistent with findings from Stephens et al. showing formaldehyde was the highest ranked carcinogen among many VOCs emitted from ENDS uses[94]. Our integrative metabolome-wide network association analysis revealed that only formaldehyde from secondhand emission, not firsthand emission, was associated with major vitamins and lipid regulated pathway perturbation. Notably, the increasing trending pattern between saliva leukotriene D4 and formaldehyde, together with the decreasing trending pattern between saliva retinoate and formaldehyde, further suggested the contribution of formaldehyde to salivary metabolic perturbation and elevated cancer risk identified with metabolite-disease network analysis. Taken together, our results indicate exposure to secondhand emission could cause considerable health risks, even at lower exposure level.

In the context of this study, it's important to note several limitations. First, the small sample sizes in this study due to the time, cost, and manpower constraints that are common to omics studies likely reduced statistical power to detect associations, especially after stratifying for puff volume-specific models. Presently, a follow-up study with a larger number of participants is ongoing, however, this current evaluation demonstrates the need to examine ENDS users based on exposures dictated by differences in puff volume. With the larger scale study, we will have sufficient power to assess specific factors such as sex and race within each puff volume group. The second limitation is the lack of metabolite validation. Future study will need to consider validating those selected metabolites as potential biomarkers by establishing in-house reference standards. Nevertheless, pathway enrichment analysis using mummichog and metabolome-wide data integration using xMWAS provide powerful solutions for analyzing data from high-resolution, untargeted metabolomics, predicting functional pathways bypassing metabolite identification, and generating high-quality, data-driven hypotheses[43,51]. Although our data describe molecular alterations due to inhalation of ENDS emissions there is a need to evaluate impacts on lung physiological function. Therefore, spirometry is being employed in the ongoing follow-up study as our current evaluation suggests the potential for functional variations associated with ENDS usage. Even given the limitations of the study, we were able to assess the metabolic reprograming and inhalation risks that were likely dependent on vaping behavior as demonstrated in this study. Rigorous statistical criteria were employed to select metabolite candidates, and further use for pathway enrichment analyses. Paired correlation analyses with stringent selection criteria (correlation threshold at $|r| > 0.64$, $p < 0.05$) were also performed to identify potential correlations between particle/VOC emissions and metabolic pathways.

Conclusion

Salivary samples from ENDS users showed significant alteration in metabolic processes, including energy metabolisms, amino acids, and lipid regulated pathways. Genome-scale reconstruction suggests that the observed metabolic perturbation in saliva was linked to several diseases including lung cancer and asthma. It is important to note that similar level of health risks may occur in populations, especially within vulnerable populations (children aged < 11 years), exposed to secondhand vaping emissions, as our results indicate a significant decrease in particle size, therefore increase in respiratory PM deposition fraction and particle associated metabolic perturbation, and comparable VOC exposure risks in secondhand exposure scenarios, particularly with use of greater puff volume by ENDS users. Although at lower emission level, formaldehyde is the most concerning VOC that possesses high cancer risk (11.3 in 1,000,000 in medium puff group and 10.3 in 1,000,000 in high puff

group from secondhand emission), which are higher than acceptable risk level (1 in 1,000,000) from US EPA. Our results also highlight that puff volume is a key vaping exposure and health risk mediator and should be further explored for ENDS regulation. Specifically, by requiring manufacturers to develop ENDS formats that limit the user's puff volume and flow rate, which are not dependent on device format or brand, participant sex, or age, could reduce exposure and thereby minimize the potential health burden of vaping.

Data availability

The authors confirm that the data supporting the findings of this study are available within the article and its Supplementary Information.

Received: 6 June 2024; Accepted: 12 August 2024
Published online: 15 August 2024

References

1. Traboulsi, H. *et al.* Inhalation toxicology of vaping products and implications for pulmonary health. *Int. J. Mol. Sci.* **21**, 3495 (2020).
2. Rebuli, M. E. *et al.* The E-cigarette or vaping product use—Associated lung injury epidemic: Pathogenesis, management, and future directions: An Official American Thoracic Society Workshop Report. *Ann. Am. Thorac. Soc.* **20**, 1–17 (2023).
3. Park-Lee, E. *et al.* Tobacco product use among middle and high school students—United States, 2022. *Morb. Mortal. Wkly. Rep.* **71**, 1429–1435 (2022).
4. King, B. A., Jones, C. M., Baldwin, G. T. & Briss, P. A. The EVALI and youth vaping epidemics—Implications for public health. *N. Engl. J. Med.* **382**, 689–691 (2020).
5. Cullen, K. A. *et al.* E-cigarette use among youth in the United States, 2019. *JAMA* **322**, 2095–2103 (2019).
6. Health UDo, and Services H. *E-Cigarette Use Among Youth and Young Adults: A Report of the Surgeon General* (2016).
7. National Academies of Sciences E, and Medicine. *Public Health Consequences of E-Cigarettes* (2018).
8. Travis, N. *et al.* Chemical profiles and toxicity of electronic cigarettes: An umbrella review and methodological considerations. *Int. J. Environ. Res. Public Health* **20**, 1908 (2023).
9. Jeon, J. *et al.* Toxicological assessment of particulate and metal hazards associated with vaping frequency and device age. *Toxics* **11**, 155 (2023).
10. Zhang, Q. *et al.* Characterization of an electronic nicotine delivery system (ENDS) aerosol generation platform to determine exposure risks. *Toxics* **11**, 99 (2023).
11. Olmedo, P. *et al.* Metal concentrations in e-cigarette liquid and aerosol samples: The contribution of metallic coils. *Environ. Health Perspect.* **126**, 027010 (2018).
12. Lee, M.-S., LeBouf, R. F., Son, Y.-S., Koutrakis, P. & Christiani, D. C. Nicotine, aerosol particles, carbonyls and volatile organic compounds in tobacco-and menthol-flavored e-cigarettes. *Environ. Health* **16**, 1–10 (2017).
13. Walley, S. C., Wilson, K. M., Winickoff, J. P. & Groner, J. A public health crisis: Electronic cigarettes, vape, and JUUL. *Pediatrics* **143**, 741 (2019).
14. Bravo-Gutiérrez, O. A. *et al.* Lung damage caused by heated tobacco products and electronic nicotine delivery systems: A systematic review. *Int. J. Environ. Res. Public Health* **18**, 4079 (2021).
15. Goniewicz, M. L. *et al.* Levels of selected carcinogens and toxicants in vapour from electronic cigarettes. *Tob. Control* **23**, 133–139 (2014).
16. Pankow, J. F. *et al.* Benzene formation in electronic cigarettes. *PLoS ONE* **12**, e0173055 (2017).
17. Antonini, J. M., Taylor, M. D., Zimmer, A. T. & Roberts, J. R. Pulmonary responses to welding fumes: Role of metal constituents. *J. Toxicol. Environ. Health A* **67**, 233–249 (2004).
18. Bein, K. & Leikauf, G. D. Acrolein—A pulmonary hazard. *Mol. Nutr. Food Res.* **55**, 1342–1360 (2011).
19. Li, L., Lin, Y., Xia, T. & Zhu, Y. Effects of electronic cigarettes on indoor air quality and health. *Annu. Rev. Public Health* **41**, 363–380 (2020).
20. Amalia, B. *et al.* Regulation of electronic cigarette use in public and private areas in 48 countries within the WHO European Region: A survey to in-country informants. *J. Epidemiol.* **32**, 131–138 (2022).
21. Fernández, E., Fu, M. & Martinez-Sanchez, J. *Exposure to Aerosol from Smoking-Proxy Electronic Inhaling Systems: A Systematic Review* (World Health Organization, 2016).
22. Control CfD, and Prevention. *State System E-Cigarette Fact Sheet* (2019).
23. Czogala, J. *et al.* Secondhand exposure to vapors from electronic cigarettes. *Nicotine Tob. Res.* **16**, 655–662 (2014).
24. Geiss, O., Bianchi, I., Barahona, F. & Barrero-Moreno, J. Characterisation of mainstream and passive vapours emitted by selected electronic cigarettes. *Int. J. Hyg. Environ. Health* **218**, 169–180 (2015).
25. Tayyarah, R. & Long, G. A. Comparison of select analytes in aerosol from e-cigarettes with smoke from conventional cigarettes and with ambient air. *Regul. Toxicol. Pharmacol.* **70**, 704–710 (2014).
26. Melstrom, P. *et al.* Measuring PM2.5, ultrafine particles, nicotine air and wipe samples following the use of electronic cigarettes. *Nicotine Tob. Res.* **19**, 1055–1061 (2017).
27. Schripp, T., Markewitz, D., Uhde, E. & Salthammer, T. Does e-cigarette consumption cause passive vaping? *Indoor Air* **23**, 25–31 (2013).
28. Prevention CfDCa. *National Health Interview Survey: Adult Tobacco Use Information* (2017).
29. Rodrigues, F. M. *et al.* Nasal and systemic inflammatory profile after short term smoking cessation. *Respir. Med.* **108**(7), 999–1006 (2014).
30. Mikheev, V. B. *et al.* The application of commercially available mobile cigarette topography devices for e-cigarette vaping behavior measurements. *Nicotine Tob. Res.* **22**, 681–688 (2020).
31. Perkins, K. A. & Karelitz, J. L. A procedure to standardize puff topography during evaluations of acute tobacco or electronic cigarette exposure. *Nicotine Tob. Res.* **22**, 689–698 (2020).
32. ISO. *ISO/IEC 17025: General Requirements for the Competence of Testing and Calibration Laboratories* (International Organization for Standardization, 2017).
33. Alqahtani, S., Cooper, B., Spears, C. A., Wright, C. & Shannahan, J. Electronic nicotine delivery system-induced alterations in oral health via saliva assessment. *Exp. Biol. Med.* **245**, 1319–1325 (2020).
34. Adamson, S. X. F., Wang, R., Wu, W., Cooper, B. & Shannahan, J. Metabolomic insights of macrophage responses to graphene nanoplatelets: Role of scavenger receptor CD36. *PLoS ONE* **13**, e0207042 (2018).
35. Xia, L. *et al.* Pulmonary and neurological health effects associated with exposure to representative composite manufacturing emissions and corresponding alterations in circulating metabolite profiles. *Toxicol. Sci.* **193**, 62–79 (2023).
36. Setyabrata, D. *et al.* Proteomics and metabolomics profiling of meat exudate to determine the impact of postmortem aging on oxidative stability of beef muscles. *Food Chem. X* **18**, 100660 (2023).

37. Koek, M. M., Jellema, R. H., van der Greef, J., Tas, A. C. & Hankemeier, T. Quantitative metabolomics based on gas chromatography mass spectrometry: Status and perspectives. *Metabolomics* **7**, 307–328 (2011).
38. Jääskeläinen, T. *et al.* A non-targeted LC–MS metabolic profiling of pregnancy: Longitudinal evidence from healthy and pre-eclamptic pregnancies. *Metabolomics* **17**, 20 (2021).
39. Tsugawa, H. *et al.* MS-DIAL: Data-independent MS/MS deconvolution for comprehensive metabolome analysis. *Nat. Methods* **12**, 523–526 (2015).
40. Chong, J. *et al.* Metaboanalyst 4.0: Towards more transparent and integrative metabolomics analysis. *Nucleic Acids Res.* **46**, W486–W494 (2018).
41. Li, S. *et al.* Predicting network activity from high throughput metabolomics. *PLoS Comput. Biol.* **9**, e1003123 (2013).
42. He, X. *et al.* Metabolomics of V2O5 nanoparticles and V2O5 nanofibers in human airway epithelial BEAS-2B cells. *Toxicol. Appl. Pharmacol.* **459**, 116327 (2023).
43. He, X. *et al.* Real-time exposure to 3D-printing emissions elicits metabolic and pro-inflammatory responses in human airway epithelial cells. *Toxics* **12**, 67 (2024).
44. Jarrell, Z. R. *et al.* Metabolic reprograming and increased inflammation by cadmium exposure following early-life respiratory syncytial virus infection: The involvement of protein S-palmitoylation. *Toxicol. Sci.* **197**, 186–196 (2024).
45. Smith, M. R. *et al.* Study on the relationship between selenium and cadmium in diseased human lungs. *Adv. Redox Res.* **7**, 100065 (2023).
46. He, X. *et al.* Low-dose vanadium pentoxide perturbed lung metabolism associated with inflammation and fibrosis signaling in male animal and in vitro models. *Am. J. Physiol. Lung Cell. Mol. Physiol.* **325**, 215–232 (2023).
47. Jarrell, Z. R. *et al.* Low-dose cadmium potentiates metabolic reprogramming following early-life respiratory syncytial virus infection. *Toxicol. Sci.* **188**, 62–74 (2022).
48. Jarrell, Z. R. *et al.* Firsthand and secondhand exposure levels of maltol-flavored electronic nicotine delivery system vapors disrupt amino acid metabolism. *Toxicol. Sci.* **182**, 70–81 (2021).
49. Zhou, G., Pang, Z., Lu, Y., Ewald, J. & Xia, J. OmicsNet 2.0: A web-based platform for multi-omics integration and network visual analytics. *Nucleic Acids Res.* **50**, W527–W533 (2022).
50. Brunk, E. *et al.* Recon3D enables a three-dimensional view of gene variation in human metabolism. *Nat. Biotechnol.* **36**, 272–281 (2018).
51. Uppal, K., Ma, C., Go, Y.-M., Jones, D. P. & Wren, J. xMWAS: A data-driven integration and differential network analysis tool. *Bioinformatics* **34**, 701–702 (2018).
52. USEPA. Consumer exposure model (CEM) version 2.0 (US) user guide. *Prepared for EPA by ICF Under EPA Contract #EP-W-12-010* (2017).
53. Bertrand, D. & Bricard, D. Real-time characterization of E-cigarettes use: The 1 million puffs study. *J. Addict. Res. Ther.* **6**, 1 (2015).
54. Cui, T. *et al.* PM1 exposure and spatial transmission of nicotine from the simulated second-hand vapor of pod-based electronic cigarettes. *Sci. Total Environ.* **1**, 165355 (2023).
55. Son, Y. *et al.* Investigating E-cigarette particle emissions and human airway depositions under various E-cigarette-use conditions. *Chem. Res. Toxicol.* **33**, 343–352 (2020).
56. Palmisani, J. *et al.* Evaluation of second-hand exposure to electronic cigarette vaping under a real scenario: Measurements of ultrafine particle number concentration and size distribution and comparison with traditional tobacco smoke. *Toxics* **7**, 59 (2019).
57. Lampos, S. *et al.* Real-time assessment of E-cigarettes and conventional cigarettes emissions: Aerosol size distributions, mass and number concentrations. *Toxics* **7**, 45 (2019).
58. Jiang, H., Gao, X., Gao, Y. & Liu, Y. Current knowledge and challenges of particle size measurements of mainstream E-cigarette aerosols and their implication on respiratory dosimetry. *J. Respir.* **3**, 7–28 (2023).
59. Bui, V. K. H., Moon, J.-Y., Chae, M., Park, D. & Lee, Y.-C. Prediction of aerosol deposition in the human respiratory tract via computational models: A review with recent updates. *Atmosphere* **11**, 137 (2020).
60. Su, W. C., Wong, S. W. & Buu, A. Deposition of E-cigarette aerosol in human airways through passive vaping. *Indoor Air* **31**, 348–356 (2021).
61. Ranpara, A., Stefaniak, A. B., Fernandez, E. & LeBouf, R. F. Effect of puffing behavior on particle size distributions and respiratory depositions from pod-style electronic cigarette, or vaping, products. *Front. Public Health* **9**, 750402 (2021).
62. Ko, U. W. & Kyung, S. Y. Adverse effects of air pollution on pulmonary diseases. *Tuberc. Respir. Dis. (Seoul)* **85**, 313–319 (2022).
63. Cowan, K. N. *et al.* Effect measure modification of the association between short-term exposures to PM(2.5) and hospitalizations by longs-term PM(2.5) exposure among a cohort of people with chronic obstructive pulmonary disease (COPD) in North Carolina, 2002–2015. *Environ. Health* **22**, 49 (2023).
64. Zhang, C.-Z. *et al.* Saliva in the diagnosis of diseases. *Int. J. Oral Sci.* **8**, 133–137 (2016).
65. Cui, Y. *et al.* Developments in diagnostic applications of saliva in human organ diseases. *Med. Novel Technol. Devices* **13**, 100115 (2022).
66. Bracken-Clarke, D. *et al.* Vaping and lung cancer—A review of current data and recommendations. *Lung Cancer* **153**, 11–20 (2021).
67. National Academies of Sciences E, and Medicine, Health and Medicine Division, Board on Population Health and Public Health Practice, Committee on the Review of the Health Effects of Electronic Nicotine Delivery Systems. *Public Health Consequences of E-Cigarettes* (National Academies Press, 2018).
68. Chen, W. & Chen, G. The roles of vitamin A in the regulation of carbohydrate, lipid, and protein metabolism. *J. Clin. Med.* **3**, 453–479 (2014).
69. Chen, F. *et al.* Prenatal retinoid deficiency leads to airway hyperresponsiveness in adult mice. *J. Clin. Investig.* **124**, 801–811 (2014).
70. Checkley, W. *et al.* Maternal vitamin A supplementation and lung function in offspring. *N. Engl. J. Med.* **362**, 1784–1794 (2010).
71. Arora, P., Kumar, V. & Batra, S. Vitamin A status in children with asthma. *Pediatr. Allergy Immunol.* **13**, 223–226 (2002).
72. Fritz, H. *et al.* Vitamin A and retinoid derivatives for lung cancer: A systematic review and meta analysis. *PLoS ONE* **6**, e21107 (2011).
73. Asakura, T., Ishii, Y., Chibana, K. & Fukuda, T. Leukotriene D4 stimulates collagen production from myofibroblasts transformed by TGF-β. *J. Allergy Clin. Immunol.* **114**, 310–315 (2004).
74. Smith, L. J., Kern, R., Patterson, R., Krell, R. D. & Bernstein, P. R. Mechanism of leukotriene D4-induced bronchoconstriction in normal subjects. *J. Allergy Clin. Immunol.* **80**, 340–347 (1987).
75. Casas, A. *et al.* Leukotriene D4-induced hypoxaemia in asthma is mediated by the cys-leukotriene1 receptor. *Eur. Respir. J.* **26**, 442–448 (2005).
76. Piperno, D. *et al.* Increased plasma levels of atrial natriuretic factor, renin activity, and leukotriene C4 in chronic obstructive pulmonary disease. *Chest* **104**, 454–459 (1993).
77. Bigby, T. D. The leukotriene C4 synthase gene and asthma. *Am. J. Respir. Cell Mol. Biol.* **23**, 273–276 (2000).
78. Holgate, S. T., Peters-Golden, M., Panettieri, R. A. & Henderson, W. R. Jr. Roles of cysteinyl leukotrienes in airway inflammation, smooth muscle function, and remodeling. *J. Allergy Clin. Immunol.* **111**, S18–S34 (2003).
79. Zhao, Y. D. *et al.* De novo synthesize of bile acids in pulmonary arterial hypertension lung. *Metabolomics* **10**, 1169–1175 (2014).
80. Aldhahrani, A., Verdon, B., Ward, C. & Pearson, J. Effects of bile acids on human airway epithelial cells: Implications for aerodigestive diseases. *ERJ Open Res.* **3**, 00107–02016 (2017).

81. De Luca, D., Alonso, A. & Autilio, C. Bile acid-induced lung injury: Update of reverse translational biology. *Am. J. Physiol. Lung Cell. Mol. Physiol.* **323**, 93–106 (2022).
82. Szumilas, K., Szumilas, P., Grzywacz, A. & Wilk, A. The effects of e-cigarette vapor components on the morphology and function of the male and female reproductive systems: A systematic review. *Int. J. Environ. Res. Public Health* **17**, 6152 (2020).
83. Crenshaw, M. D. *et al.* Determination of nicotine, glycerol, propylene glycol and water in electronic cigarette fluids using quantitative 1 H NMR. *Magn. Reson. Chem.* **54**, 901–904 (2016).
84. Wieslander, G., Norback, D. & Lindgren, T. Experimental exposure to propylene glycol mist in aviation emergency training: Acute ocular and respiratory effects. *Occup. Environ. Med.* **58**, 649–655 (2001).
85. Choi, H., Schmidbauer, N., Spengler, J. & Bornehag, C.-G. Sources of propylene glycol and glycol ethers in air at home. *Int. J. Environ. Res. Public Health* **7**, 4213–4237 (2010).
86. Madison, M. C. *et al.* Electronic cigarettes disrupt lung lipid homeostasis and innate immunity independent of nicotine. *J. Clin. Investig.* **129**, 4290–4304 (2020).
87. Morris, A. M. *et al.* Effects of e-cigarette flavoring chemicals on human macrophages and bronchial epithelial cells. *Int. J. Environ. Res. Public Health* **18**, 11107 (2021).
88. Dwivedi, A. M., Upadhyay, S., Johanson, G., Ernstgård, L. & Palmberg, L. Inflammatory effects of acrolein, crotonaldehyde and hexanal vapors on human primary bronchial epithelial cells cultured at air–liquid interface. *Toxicol. Vitro* **46**, 219–228 (2018).
89. LeBouf, R. F. *et al.* Chemical emissions from heated vitamin E acetate—Insights to respiratory risks from electronic cigarette liquid oil diluents used in the aerosolization of Δ9-THC-containing products. *Front. Public Health* **9**, 765168 (2022).
90. Jiang, H. *et al.* Chemical and toxicological characterization of vaping emission products from commonly used vape juice diluents. *Chem. Res. Toxicol.* **33**, 2157–2163 (2020).
91. Floss, M. A. *et al.* Exhaled aldehydes as biomarkers for lung diseases: A narrative review. *Molecules* **27**, 5258 (2022).
92. Grassin-Delyle, S. *et al.* Metabolomics of exhaled breath in critically ill COVID-19 patients: A pilot study. *EBioMedicine* **63**, 103154 (2021).
93. Lim, H. H. & Shin, H. S. Determination of volatile organic compounds including alcohols in refill fluids and cartridges of electronic cigarettes by headspace solid-phase micro extraction and gas chromatography–mass spectrometry. *Anal. Bioanal. Chem.* **409**, 1247–1256 (2017).
94. Stephens, W. E. Comparing the cancer potencies of emissions from vapourised nicotine products including e-cigarettes with those of tobacco smoke. *Tob. Control* **27**, 10–17 (2018).
95. Li, S. *et al.* Metabolic phenotypes of response to vaccination in humans. *Cell* **169**, 862–877 (2017).
96. Hagan, T. *et al.* Antibiotics-driven gut microbiome perturbation alters immunity to vaccines in humans. *Cell* **178**, 1313–1328 (2019).

Acknowledgements

The authors would like to thank Dr. Joe Hess (Chemical Insights Research Institute), Dr. Scott Weaver (School of Public Health, Georgia State University), and Dr. Ruiyan Luo (School of Public Health, Georgia State University) for their analytical contributions. They also would like to acknowledge the support of the Purdue Metabolite Profiling Facility for their technical support in generating the metabolomic data presented with the manuscript.

Author contributions

Author contributions: Conceptualization: C.W., J.S.; methodology: C.W., J.S. J.J., X.H., M.M., Z.Q.; investigation: C.W., J.S., J.J., Q.Z.; data curation: C.W., J.J., X.H., A.S., Q.Z.; writing- original draft preparation: J.J., X.H., M.M., L.B., A.S., Q.Z., M.B., J.S., C.W.; supervision: M.B, C.W.; project administration: C.W.; funding acquisition: C.W., J.S., M.B.

Funding

This work has been carried out with the coordination of National Institute of Health in the framework of the project entitled "African-American Susceptibility to Periodontal Disease due to Electronic Nicotine Delivery Systems (ENDS) Usage" (Award Number: 1R56DE029950-01A1).

Competing interests

The authors declare no competing interests.

Additional information

Supplementary Information The online version contains supplementary material available at https://doi.org/10.1038/s41598-024-69985-1.

Correspondence and requests for materials should be addressed to J.S. or C.W.